



## Using long-term daily satellite based rainfall data (1983-2015) to analyze spatio-temporal changes in the sahelian rainfall regime

Zhang, Wenmin; Brandt, Martin Stefan; Guichard, Francoise; Tian, Qingjiu; Fensholt, Rasmus

*Published in:*  
Journal of Hydrology

*DOI:*  
[10.1016/j.jhydrol.2017.05.033](https://doi.org/10.1016/j.jhydrol.2017.05.033)

*Publication date:*  
2017

*Document version*  
Peer reviewed version

*Document license:*  
[Unspecified](#)

*Citation for published version (APA):*  
Zhang, W., Brandt, M. S., Guichard, F., Tian, Q., & Fensholt, R. (2017). Using long-term daily satellite based rainfall data (1983-2015) to analyze spatio-temporal changes in the sahelian rainfall regime. *Journal of Hydrology*, 550, 427-440. <https://doi.org/10.1016/j.jhydrol.2017.05.033>

1 Using long-term daily satellite based rainfall data (1983-2015) to  
2 analyze spatio-temporal changes in the sahelian rainfall regime

3  
4 Wenmin Zhang<sup>a,b</sup>, Martin Brandt<sup>b</sup>, Françoise Guichard<sup>c</sup>, Qingjiu Tian<sup>a</sup>, Rasmus Fensholt<sup>b</sup>

5 *<sup>a</sup>International Institute for Earth System Sciences, Nanjing University, 210023 Nanjing,*

6 *China*

7 *<sup>b</sup>Department of Geosciences and Natural Resource Management, University of Copenhagen,*

8 *1350 Copenhagen, Denmark*

9 *<sup>c</sup>Centre Nationale de Recherches Météorologiques (CNRM), Météo-France & UMR CNRS*

10 *3589, 42 Avenue Gaspard Coriolis, 31100 Toulouse, France*

11

12 **ABSTRACT:**

13 The sahelian rainfall regime is characterized by a strong spatial as well as intra- and inter-annual  
14 variability. The satellite based African Rainfall Climatology Version 2 (ARC2) daily gridded rainfall estimates  
15 with a  $0.1^\circ \times 0.1^\circ$  spatial resolution provides the possibility for in-depth studies of seasonal changes over a 33-  
16 year period (1983 to 2015). Here we analyze rainfall regime variables that require daily observations: onset,  
17 cessation, and length of the wet season; seasonal rainfall amount; number of rainy days; intensity and frequency  
18 of rainfall events; dry spell frequency, length, and cumulative duration. Rain gauge stations and MSWEP  
19 (Multi-Source Weighted-Ensemble Precipitation) data were used to evaluate the agreement of rainfall variables  
20 in both space and time, and trends were analyzed. Overall, ARC2 rainfall variables reliably show the spatio-  
21 temporal dynamics of seasonal rainfall over 33 years when compared to gauge and MSWEP data. However, a  
22 higher frequency of low rainfall events ( $<10 \text{ mm day}^{-1}$ ) is found for satellite estimates as compared to gauge  
23 data, which also causes disagreements between satellite and gauge based variables due to sensitivity to the  
24 number of days with observations (frequency, intensity, and dry spell characteristics). Most rainfall variables  
25 (both ARC2 and gauge data) show negative anomalies (except for onset of rainy season) from 1983 until the  
26 end of the 1990s, from which anomalies become mostly positive and inter-annual variability is higher. ARC2  
27 data show a strong increase in seasonal rainfall, wet season length (caused by both earlier onset and a late end),

---

\*Corresponding author at: Oester Voldgade 10, 1350 Copenhagen, Denmark.  
E-mail address: wenminzhg@gmail.com

28 number of rainy days, and high rainfall events ( $>20 \text{ mm day}^{-1}$ ) for the western/central Sahel over the period of  
29 analysis, whereas the opposite trend characterizes the eastern part of the Sahel.

30

31 *Keywords: ARC2; daily observations; rain gauge; rainfall regime; Sahel; spatio-temporal*  
32 *analysis*

33

## 34 **1. Introduction**

35 The Sahel is known as one of the largest semi-arid regions in the world and  
36 livelihoods of the sahelian rural population depend primarily on rain-fed agriculture and  
37 livestock farming (Leisinger and Schmitt, 1995). The Sahel zone is characterized by high  
38 intra-annual variability, affecting water resources and food security (Le Barbé et al., 2002;  
39 Nicholson, 1993, 1989; Nicholson and Palao, 1993). The region has experienced several  
40 decades of abnormally dry conditions over the past 50 years, including two sequences of  
41 extremely dry years in 1972-1974 and 1983-1985 (Hulme, 1992; Le Barbé and Lebel, 1997).  
42 These periods, well known as the Sahel droughts, caused severe famines, human and  
43 livestock deaths, land abandonment, and large-scale migrations. Sahelian sedentary farmers  
44 and pastoralists are consequently forced to adapt to the general decrease in water resources  
45 and increase in rainfall variability (Mortimore and Adams, 2001; Romankiewicz et al., 2016).  
46 Water availability and timing of precipitation events are key factors for the agricultural crop  
47 production (Berg et al., 2009; Sultan et al., 2005) and primary productivity of herbaceous and  
48 woody vegetation in the Sahel (Huber et al., 2011). The timing of start of the wet season is  
49 pivotal, as most farmers and pastoralists form decisions on cropping and livestock  
50 movements on the basis of the occurrence of the first rains (Ingram et al., 2002). Finally, the  
51 timing of the seasonal rainfall is decisive; e.g., late season rainfall may lead to high  
52 annual/seasonal rainfall sums, however being of little use for crops and herbaceous  
53 vegetation, which are both photoperiodic (Breman and Kessler, 2012). Any changes in the

54 overall rainfall regime will have profound impacts on livelihoods. However, the network of  
55 rain gauge stations in Africa, and particularly in the Sahel, has decreased significantly in  
56 recent years (Eklund et al., 2016; Sanogo et al., 2015), adding considerable uncertainty to  
57 datasets based on station data only (e.g., the CRU (Climate Research Unit) rainfall datasets)  
58 and analyzes hereof (Eklund et al., 2016), hampering studies of rainfall regime changes.  
59 Moreover, the Sahel rainfall spatial heterogeneity is not well captured by the gridded CRU  
60 datasets (0.5 ° spatial resolution) or by widely dispersed station data from gauge observations.  
61 Seasonal rainfall is found to vary significantly at scales of a few tens of km (meso-scale)  
62 (Nicholson, 2000) and spatial variability at the daily timescales is also high due to the  
63 predominantly convective nature of precipitation during the rainy season (Lebel et al., 2003;  
64 Laurent et al., 1998)

65         Precipitation estimates from satellites provide repetitive, timely, objective, and cost-  
66 effective information on the spatio-temporal distribution of rainfall. Estimates of with a high  
67 spatio-temporal resolution have been available for the African continent since the 1980s from  
68 the METEOSAT satellites and provide vital information on rainfall in areas with an  
69 insufficient station network (Maidment et al., 2015). A variety of rainfall datasets have been  
70 produced using convective cloud top temperature and by applying the cold cloud duration  
71 (CCD) technique (Adler et al., 1994). The performance varies considerably, and calibration  
72 and evaluations using rain gauges of such CCD based satellite rainfall products are critical  
73 (Jobard et al., 2011; H Laurent et al., 1998; Love et al., 2004; Nicholson et al., 2003a,  
74 2003b). An acceptable agreement is often found between satellite and gauge data, even  
75 though inter-annual variations in bias are commonly found (McCollum et al., 2000;  
76 Nicholson et al., 2003a, 2003b). Yet, the satellite data used in these studies mostly covers  
77 relatively short periods of time and only decadal or monthly rainfall observations are  
78 evaluated (Moron, 1994; Nicholson and Palao, 1993; Sanogo et al., 2015; Maidment et al.,

79 2015). Only two recent studies have analyzed the satellite/gauge relationship on a daily scale  
80 over Sahel (Dembélé and Zwart, 2016; Sanogo et al., 2015), both reporting a moderate  
81 agreement ( $r^2$  below 0.3) between satellite and gauge data.

82 Advances have been made in understanding the regional circulations and their  
83 relationships to water vapour transport in the West African region (Thorncroft et al., 2011).  
84 However, most studies of changes in the sahelian rainfall define the rainy season as a fixed  
85 set of months (from either gauge or satellite data) (Jobard et al., 2011; Nicholson, 2005;  
86 Nicholson et al., 2003a, 2003b; Sealy et al., 2003). The four months from June to September  
87 are usually considered as the rainy season since more than 80% of the annual rainfall falls  
88 during this period (Lebel et al., 2003; Sanogo et al., 2015). Only a few scholars have studied  
89 changes in the Sahel rainfall regime based on variables such as onset and cessation of the  
90 rainy season, rainy days, rainfall intensity from gauge/satellite data (Nicholson and Palao,  
91 1993; Sanogo et al., 2015; Dunning et al., 2016) that can only be resolved using daily rainfall  
92 data.

93 In this study we evaluate the use of the satellite based Africa rainfall climatology  
94 version 2 (ARC2) dataset (Novella and Thiaw, 2012) (available from 1983 to the present at  
95 daily time steps with a  $0.1^\circ \times 0.1^\circ$  spatial resolution) in the characterization of the Sahel  
96 rainfall regime and changes herein. The high temporal and spatial resolution enables a  
97 comprehensive study of spatially distributed rainfall variables describing the rainfall regime  
98 (onset and cessation dates, length of the wet season, seasonal rainfall amount, rainy day,  
99 intensity and frequency of rainfall events, dry spell characteristics (frequency, intensity, and  
100 cumulative dry days of dry spells)). All variables are validated against rain gauge data over a  
101 33-year period. The robustness of the ARC2 rainfall metrics and furthermore intercompared  
102 with the global coverage MSWEP dataset (Beck et al., 2017) produced also with a daily  
103 temporal resolution. The objectives of this study are threefold: (1) to evaluate the agreement

104 between rainfall variables derived from ARC2, MSWEP and available long-term continuous  
105 rain gauge data of daily resolution; (2) to analyze selected ARC2 and gauge derived variables  
106 over the full time period; (3) to study the spatial variability in temporal trends of ARC2  
107 derived variables.

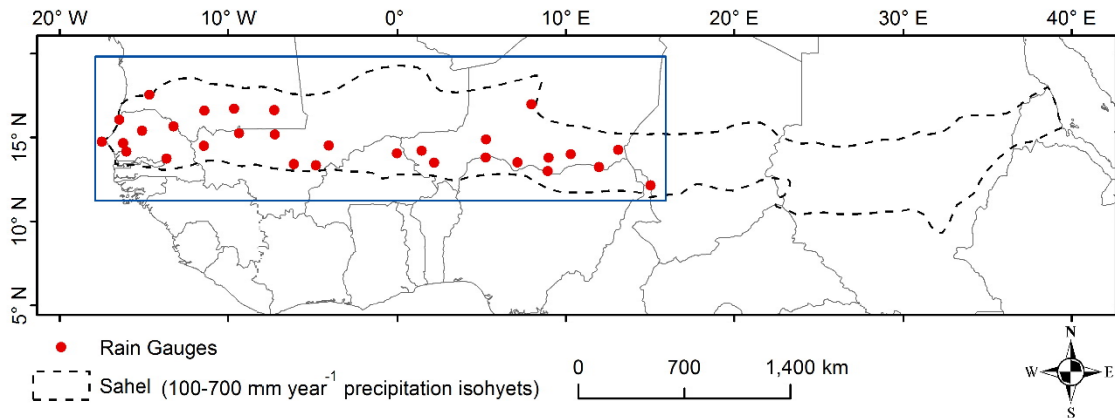
108

## 109 **2. Materials and methods**

### 110 *2.1 Study area*

111 The Sahel extends from the Atlantic Ocean in the west to the Red Sea in the east and  
112 constitutes a transition zone between the arid northern and the humid southern eco-regions  
113 (Fig.1). The delineation was derived from the ARC2 average annual rainfall (1983-2015)  
114 with northern/southern boundaries of 100 mm and 700 mm, respectively (Lebel et al., 2009).  
115 Typically, the rainy season lasts from June to early October with a peak in August (Le Barbé  
116 and Lebel, 1997) and is characterized by a high inter-annual variability, with a coefficient of  
117 variation of the mean annual rainfall ranging from 15% to 30% (Sivakumar, 1989). The  
118 climate is directly linked to the West African Monsoon with a decreasing rate of annual  
119 rainfall of approximately  $1 \text{ mm km}^{-1}$  along a south-north gradient (Lebel et al., 1997;  
120 Frappart et al., 2009). The comparison between ARC2 rainfall and gauge measurements  
121 focuses on western and central parts of the Sahel, where the availability of gauge  
122 measurements without substantial data gaps is more abundant as compared to the eastern  
123 Sahel.

124



125

126 **Fig. 1 .** Study area (Sahel) with 100–700 mm year<sup>-1</sup> precipitation isohyets (ARC2 mean annual rainfall, 1983–  
 127 2015) and rain gauges included in this study. Blue rectangle outlines the area used for analysis in Fig.S7.

128

129 *2.2 Datasets*

130 *2.2.1 ARC2 dataset*

131 The ARC2 (African Rainfall Climatology Version 2) satellite based daily rainfall  
 132 dataset is available from 1983–present at a 0.1° × 0.1° spatial resolution (approximately  
 133 11 × 11 km). ARC2 builds on ARC1 that is developed using the algorithm applied in the RFE2  
 134 (Rainfall Estimation version 2) which is found to be amongst the most reliable products of  
 135 satellite based datasets covering Africa (Love et al., 2004). The difference as compared to  
 136 RFE2 is that ARC1 uses only gauge and infra-red data whereas RFE2 uses additional  
 137 microwave data, which is not available prior to 1995 (Love et al., 2004). Ultimately, ARC2 is  
 138 a revision of ARC1 with a recalibration of the 1983 to 2005 period (Novella and Thiaw,  
 139 2012).

140 *2.2.2 MSWEP dataset*

141 The global coverage MSWEP (Multi-Source Weighted-Ensemble Precipitation,  
 142 version 1.2) rainfall dataset is provided with 3-hour temporal resolution for the period 1979–  
 143 2015 in a 0.25° spatial resolution (Beck et al., 2017). MSWEP is developed by merging the  
 144 highest quality precipitation data sources available as a function of timescale and location

145 from the combined use of rain-gauge measurements, satellite observations, and estimates  
146 from atmospheric models (Beck et al., 2017).

### 147 *2.2.3 Rain gauge dataset*

148 The gauge rainfall is derived from the Global Historical Climatology Network  
149 (GHCN-Daily) (Menne et al., 2012). GHCN rainfall measurements from rain gauge stations  
150 are considered to be the most accurate and reliable source of precipitation data in the region  
151 (Durre et al., 2010). Stations with at least 80% data availability throughout the entire period  
152 1983–2015 were selected as references for the comparison to ARC2 data, leading to the  
153 selection of 30 stations distributed from 17°W to 15°E (Fig.1). No gap-filling of missing  
154 daily observations was done. When a record is missing at a given station, the corresponding  
155 ARC2 record is discarded to provide the most accurate comparison of datasets.

### 156 *2.3 Variables describing the rainfall regime*

157 Variables based on daily rainfall were defined to characterize the rainfall regime  
158 (Table 1). Several definitions of onset and end of season exist, based on thresholds of the  
159 amount of rainfall recorded during consecutive days (Marteau et al., 2009; Omotosho et al.,  
160 2000; Sivakumar, 1988). Fitzpatrick et al. (2015) compared the onset dates calculated from  
161 different definitions, datasets, and resolutions and found these choices to have a strong  
162 impact on the local patterns of onset dates. To find a criterion that fits both ARC2 and gauge  
163 data, we modified the definition proposed by Fitzpatrick et al. (2015) moderately. We defined  
164 the onset as the first occurrence of at least 20 mm cumulative rainfall within 7 days after May  
165 1, followed by a total of 20 mm rainfall within the next 20 days (to avoid including so-called  
166 “false starts”, which do not cause the start of growing season). We determined the end of the  
167 rainy season by the occurrence of 20 consecutive days with cumulated rainfall less than 10  
168 mm after September 1. Length of the rainy season was defined as the number of days  
169 between the onset and cessation of the rainy season.



170 The amount of seasonal rainfall was calculated by summing the daily rainfall events  
 171  $\geq 1$  mm within a rainy season. The number of rainy days was calculated for different levels of  
 172 intensity: 1–10, 10–20, 20–30, and greater than 30 mm day<sup>-1</sup>. The intensity of rainfall was  
 173 calculated by dividing the amount of rainfall within the rainy season by the number of rainy  
 174 days. To characterize dry spells within a rainy season, three variables were calculated: the  
 175 dry spell frequency, length and cumulative dry days (definitions provided in Table 10).  
 176 Seasonal distribution of the rainfall over the wet season was calculated from the ratio of the  
 177 rainfall between the first and second half of the season.

178

179

**Table 1** Summary of rainfall variables applied

<b>Variables</b>	<b>Definitions</b>
Onset of rainy season	The first occurrence of at least 20 mm cumulative rainfall within 7 days after May 1, followed by a total of 20 mm rainfall within the next 20 days.
Cessation of rainy season	The occurrence of 20 consecutive days with cumulated rainfall less than 10 mm after September 1.
Length of rainy season	Number of days between the onset and the cessation of the rainy season
Seasonal rainfall amount	Rainfall amount during the rainy season.
Rainy day	Number of rainy days ( $\geq 1$ mm day <sup>-1</sup> ) between the onset and cessation.
Frequency	The percent of rainy days: the number of rainy days/length of rainy season.
Intensity	Amount of rainfall within the rainy season amount/the number of rainy days.
Seasonal distribution	Ratio of rainfall between the first and second half of the wet season (50% of length of season).
Dry Spell	Rainfall $< 1$ mm day <sup>-1</sup> during a period of at least seven consecutive days.
Frequency of dry spell	The number of dry spells during rainy season.
Length of dry spell	Mean length of dry spells.
Cumulative dry days	The total number of dry days accumulated over all dry spells in a rainy season.

180

## 181 *2.4 Methodology*

182 Both individual 0.1° ARC2 pixels overlaying the rain gauge stations (Fig. 1) and a 3×3  
 183 pixel window (Fig.S1) were initially tested for the comparison. As the results were nearly  
 184 identical, only the single pixel overlap method was selected for presentation as this is  
 185 expected to minimize the bias induced by the scale difference between points and pixels.

186 ARC2 pixels were aggregated to match the MSWEP spatial resolution for the  
 187 intercomparison of satellite based products.

#### 188 2.4.1 Standardized rainfall index

189 Anomalies based on a standardized rainfall index were used to quantify each rainy  
 190 season in relation to the long-term climatology. Rainfall anomalies are normally computed by  
 191 averaging the standardized annual variables recorded at each rain gauge station available for  
 192 a given year (Lamb, 1982; Nicholson, 1985). However, due to the strong spatial variability of  
 193 the sahelian rainfall and the uneven distribution of the rain gauge network, we applied the  
 194 index proposed by Ali and Lebel (2009) for any variable  $V$  ( e.g., seasonal rainfall, onset...),  
 195 being a function of  $n$  for site and  $y$  for year:

$$196 \quad \sigma_{\sigma}(n, y) = \frac{\sigma(n, y) - \sigma(n)}{\sigma[\sigma(n)]}$$

197 where  $\sigma_{\sigma}(n, y)$  is the  $V$  index,  $\sigma(n)$  and  $\sigma[\sigma(n)]$  are the mean and standard  
 198 deviation, respectively, of  $V$  over the region and the reference period 1983-2015. Region  
 199 refers here to all the rain gauge stations shown in Fig.1.

#### 200 2.4.2 Data analysis

201 To characterize the consistency of rainfall variables between ARC2, MSWEP and  
 202 gauge data, the linear correlation were performed with Pearson's *t-test*. The correlation  
 203 analysis was conducted on detrended data (significant linear trends ( $p < 0.05$ ) in rainfall  
 204 variables were removed) to avoid spurious correlations. Trends were estimated using Sen's  
 205 slope and assessed with Mann-Kendall test accounting for the effect of serial correlation.  
 206 Continuous wavelet analysis was conducted on detrended data to assess changes in rainfall  
 207 variables as a function of time-scales ranging from inter-annual to decadal variability.

208 Temporal trend analysis was performed to detect changes in trends of rainfall variables  
209 including all combinations of sub-periods with a minimum period length of 10 years.

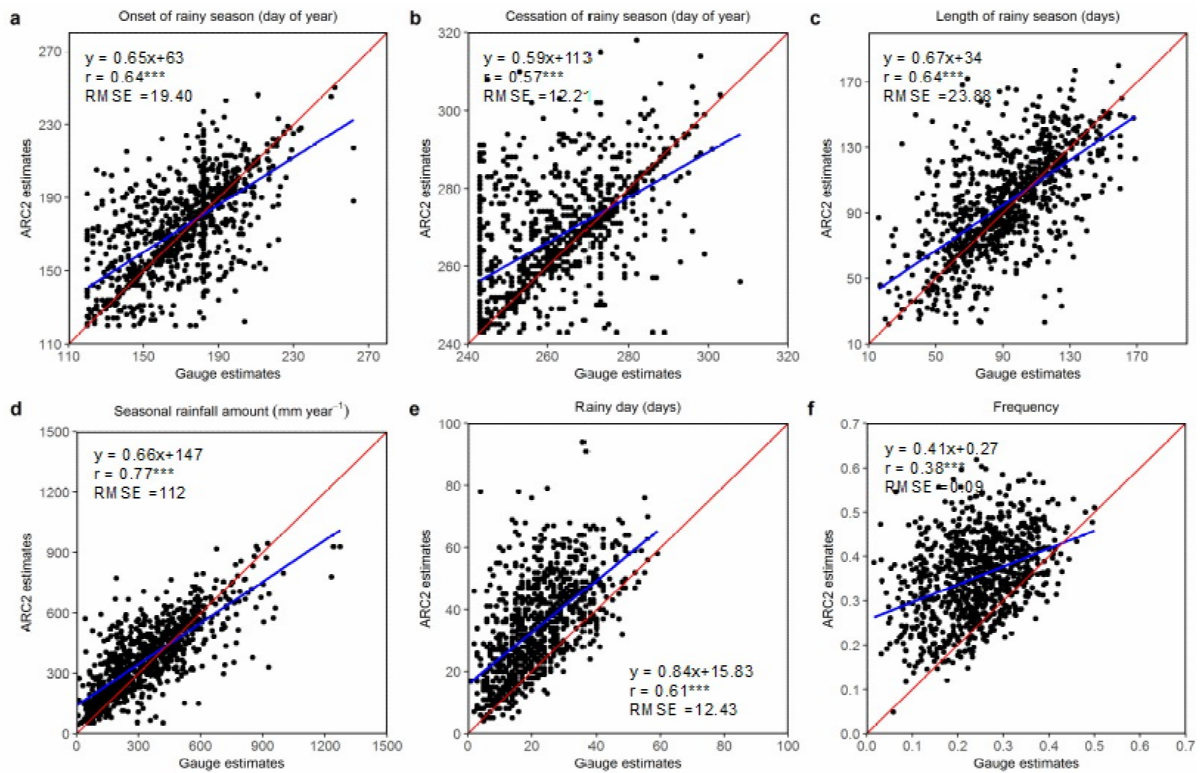
### 210 **3. Results**

#### 211 *3.1 Spatio-temporal correlations between rain gauges and ARC2*

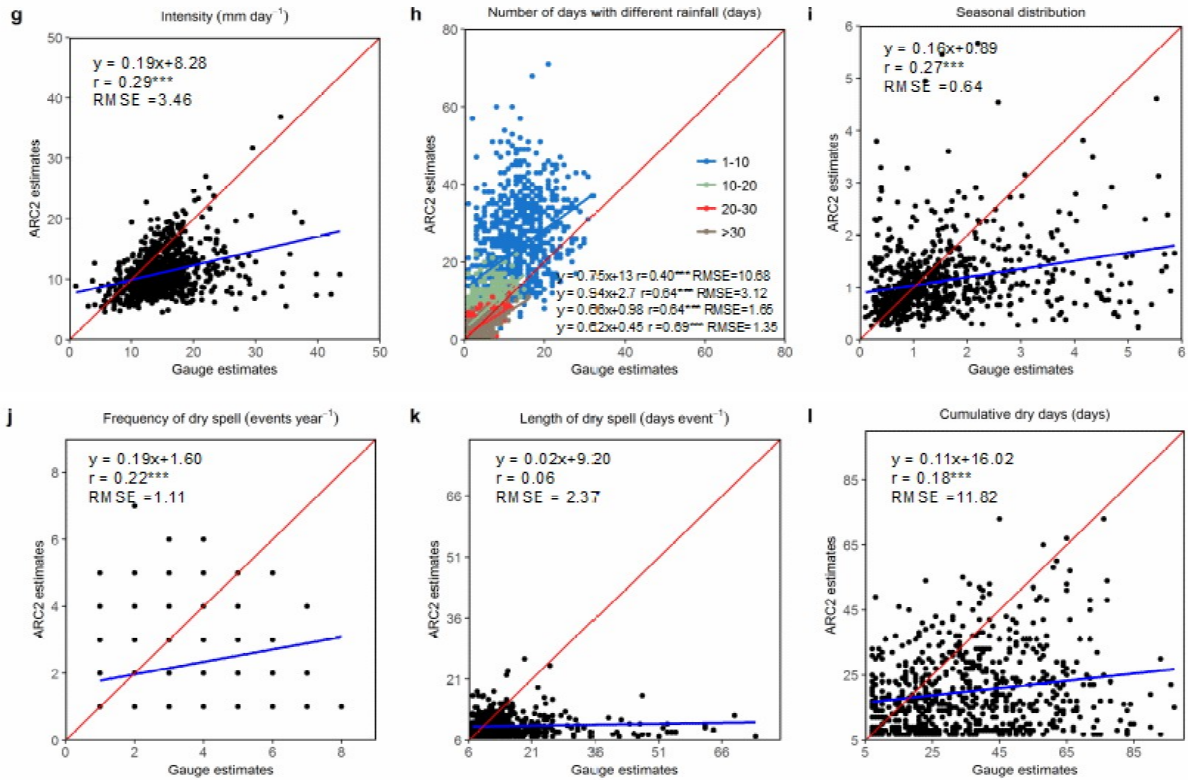
212 Spatio-temporal correlations between rain gauge and ARC2 data were examined by  
213 successively analyzing: (i) the rainfall variables across the rain gauge sites; and (ii) the time  
214 series of annual standardized seasonal rainfall averaged over the sites.

215 The comparison of the 33-year seasonal rainfall variables indicates a fair linear  
216 relationship between ARC2 and rain gauges for all variables (r values between 0.29 and 0.77)  
217 except the dry spell variables with r values between 0.06-0.22) (Fig.2). The onset, cessation,  
218 length of the rainy season and the seasonal rainfall amount generally correspond well (Fig.2a-  
219 d). A strong discrepancy is observed in the occurrence of rainfall events lower than 20 mm  
220 day<sup>-1</sup> (1-10 and 10-20 mm day<sup>-1</sup>) (Fig.2h), with a pronounced higher number of days of  
221 observations in the satellite product as compared to gauge measurements. The higher  
222 frequency of satellite rainfall events becomes smaller for events of higher rainfall (20-30 mm  
223 day<sup>-1</sup>) and a lower frequency of the number of strong ARC2 rainfall events (> 30 mm day<sup>-1</sup>)  
224 is observed (Fig.2h). The higher representation of low rainfall from the satellite also results in  
225 a higher satellite based number and frequency of rainy days (Fig.2e-f) and correspondingly  
226 lower values of satellite based rainfall intensity (Fig.2g). While the satellite seasonal rainfall  
227 amounts are close to gauge measured rainfall, the observed correspondence includes much  
228 more frequent low rainfall events and slightly less frequent strong rainfall events (Fig.S2  
229 supplementary information). ARC2 versus gauge based seasonal distribution (Fig.2i)  
230 indicates a bias towards more gauge based occurrences of early season rainfall as compared  
231 to satellite rainfall. Comparison of satellite and gauge based estimates of dry spell  
232 characteristics (Fig.2j-l) is severely impacted by the higher frequency of satellite based

233 records of low rainfall events, causing much higher gauge based dry spell frequencies,  
 234 lengths and cumulative dry days. Similar results are obtained when analyzing 33-year  
 235 average values of rainfall variables (Fig.S3).  
 236



237



238

239 **Fig. 2.** Scatterplots between annual ARC2 (individual ARC2 pixels overlaying rain gauge stations) and gauge  
 240 rainfall variables (1983-2015) for all sites (shown in Fig.1). The blue line is the linear regression line between  
 241 gauge and ARC2 estimates (except for Fig.2h) and the red line is the 1:1 line. Linear correlation coefficients ( $r$ )  
 242 between ARC2 and gauge rainfall variables are shown and asterisks denote significant correlations ( $*=p < 0.1$ ;  
 243  $**=p < 0.05$ ;  $***=p < 0.01$ ). DETAILS: a) onset of rainy season (day of year); b) cessation of rainy season (day  
 244 of year); c) length of rainy season (days); d) seasonal rainfall amount (mm year<sup>-1</sup>); e) rainy day (days); f)  
 245 frequency; g) intensity (mm year<sup>-1</sup>); h) number of days with rainfall 1-10, 10-20, 20-30, >30 mm day<sup>-1</sup> (days); i)  
 246 seasonal distribution; j) frequency of dry spell (events year<sup>-1</sup>); k) length of dry spell (days events<sup>-1</sup>); l)  
 247 cumulative dry days (days).

248

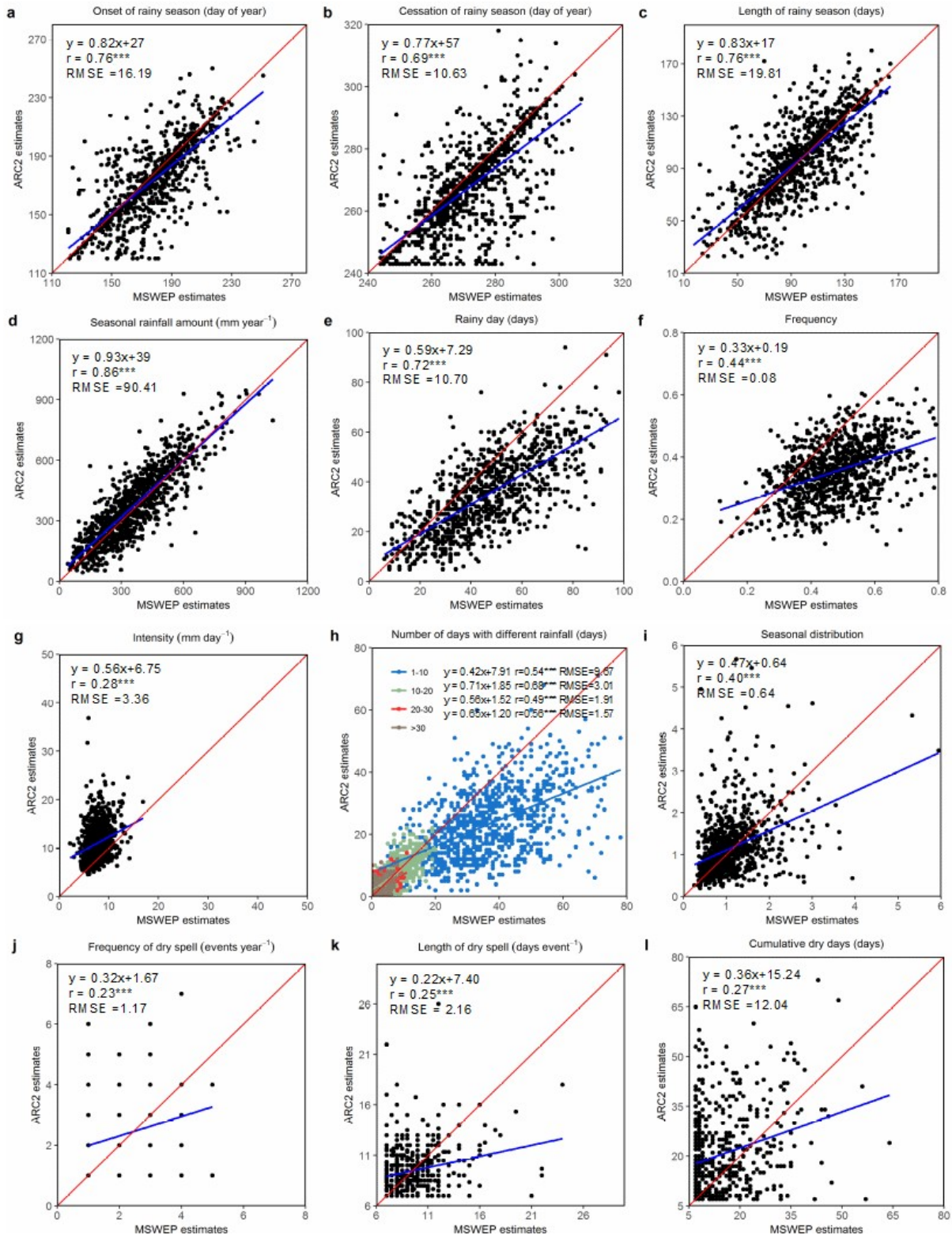
249 ARC2 derived rainfall variables were compared with corresponding metrics derived  
 250 from MSWEP (Fig.3). Overall, a good consistency between ARC2 and MSWEP rainfall  
 251 metrics was observed for rainfall seasonal timing and seasonal amount (Fig.3a-d) with  $r$   
 252 values ranging between 0.69 and 0.86. For the metrics related to the timing/frequency of  
 253 individual rainfall events (Fig.3e,f,h) there is a bias towards more observations from MSWEP  
 254 as compared to ARC2 (especially pronounced for rainfall events of 1-10 mm day<sup>-1</sup>) causing

255 the calculation of rainfall intensity to be higher for ARC2 as compared to MSWEP (Fig.3g).

256 The difference in frequency of rainfall events causes the dry spell comparisons to show

257 moderate agreement ( $r$  values between 0.23 and 0.27) (Fig.3j-l).

258



259



260 **Fig. 3.** Scatterplots between annual ARC2 and MSWEP rainfall variables (1983-2015) for all sites (shown in  
261 Fig.1). The blue line is the linear regression line between gauge and ARC2 estimates (except for Fig.3h) and the  
262 red line is the 1:1 line. Linear correlation coefficients ( $r$ ) between ARC2 and gauge rainfall variables are shown  
263 and asterisks denote significant correlations ( $*=p < 0.1$ ;  $**=p < 0.05$ ;  $***=p < 0.01$ ). DETAILS: a) onset of rainy  
264 season (day of year); b) cessation of rainy season (day of year); c) length of rainy season (days); d) seasonal  
265 rainfall amount ( $\text{mm year}^{-1}$ ); e) rainy day (days); f) frequency; g) intensity ( $\text{mm year}^{-1}$ ); h) number of days with  
266 rainfall 1-10, 10-20, 20-30,  $>30 \text{ mm day}^{-1}$  (days); i) seasonal distribution; j) frequency of dry spell (events year  
267  $^{-1}$ ); k) length of dry spell ( $\text{days events}^{-1}$ ); l) cumulative dry days (days).

268

### 269 *3.2 Inter-annual variability and trends of rain gauge and ARC2 variables*

270 The temporal consistency of rainfall variables over the 33-year period for both gauge  
271 and ARC2 (Fig.4) was assessed using the correlation coefficients and statistical significance  
272 was determined by Pearson's *t-test* accounting for serial correlation (Table 2). The results are  
273 generally in line with those obtained for the spatial correlations (Fig.2 and Fig.S3), with the  
274 weakest agreement (both ARC2/gauge and ARC2/MSWEP) between data for low rainfall  
275 events, intensity, and seasonal distribution. However, the ARC2/gauge correlations of dry  
276 spell variables are higher when averaged over time than over space, which suggests that  
277 ARC2 better captures inter-annual than spatial fluctuations of dry spells. Clear positive trends  
278 are shown in the rainy season length, the seasonal rainfall amount, the number of rainy days,  
279 the rain event frequency, and the rainy days above  $10 \text{ mm day}^{-1}$  (10-20, 20-30 and  $>30 \text{ mm}$   
280  $\text{day}^{-1}$ ) in both ARC2, MSWEP and gauge data (Table 2). Temporal consistency between  
281 ARC2 and MSWEP is found with significant correlations for all rainfall variables during  
282 1983-2015. However, significant trends of MSWEP are only found for cessation, length of  
283 rainy season, seasonal rainfall amount, intensity and number of days with rainfall of 10-20  
284 and  $20\text{-}30 \text{ mm day}^{-1}$ , whereas also the onset, number of rainy days, number of days with  
285 rainfall of  $>30 \text{ mm day}^{-1}$  and seasonal distribution are characterized by significant trends for  
286 ARC2.

287 Negative anomalies dominated from 1983 to the end of the 1990s, while after this  
288 period, more consistent positive anomalies from 2000 to present were observed (Fig.4c-k).  
289 The increase in rainy season length associated with a significantly negative trend in the onset  
290 dates of the rainy season is found in both ARC2 and gauge (Fig.4a and c). Rain gauge data  
291 indicates significantly positive trend in the number of rain events from the small (1-10 mm  
292 day<sup>-1</sup>) to the high (>30 mm day<sup>-1</sup>), which agrees with the results of ARC2, except for the  
293 trend of small rainfall events (not significant for ARC2) (Table 2). The ARC2 based rainfall  
294 intensity is characterized by a significantly positive trend, which is not supported by the  
295 gauge data (Fig.4g and Table 2). It is noticeable that no significant trends are observed for  
296 dry spells in both datasets despite the strong positive trend of seasonal rainfall (Fig.4m-o and  
297 Table 2); i.e., the partial recovery of rainfall observed since the 80s' droughts is not  
298 associated with a substantial decrease of dry spells during the monsoon. A significantly  
299 negative trend is seen in the seasonal distribution for ARC2 (showing a shift in the ratio  
300 between early and late rainfall towards later monsoon rainfall) while no change is observed in  
301 gauges (Table 2). Wavelet analysis of rainfall variables from both ARC2 and rain gauges  
302 show that inter-annual variability of all rainfall metrics appears to be dominated by shorter  
303 year-to-year fluctuations (Fig.5 and Fig.S5). Strong inter-annual fluctuations are observed in  
304 in several variables, e.g., the onset and cessation dates (Fig .5a-b). A higher inter-annual  
305 variability in seasonal rainfall amount and the number of rainy days (10-20, 20-30, and >30  
306 mm day<sup>-1</sup>) is also observed over the past 15 years as compared to the beginning of the time  
307 series (Fig.5d, h-k). Multi-year fluctuations could also be identified for variables of the  
308 seasonal timing (Fig.5a-c).

309 Trends in ARC2 rainfall variables for various time scale combinations (multi-  
310 temporal trend analysis) were determined by Mann–Kendall's tau value (only considering  
311 direction) (Fig.6). Significantly negative trends are dominating for the onset of rainy season



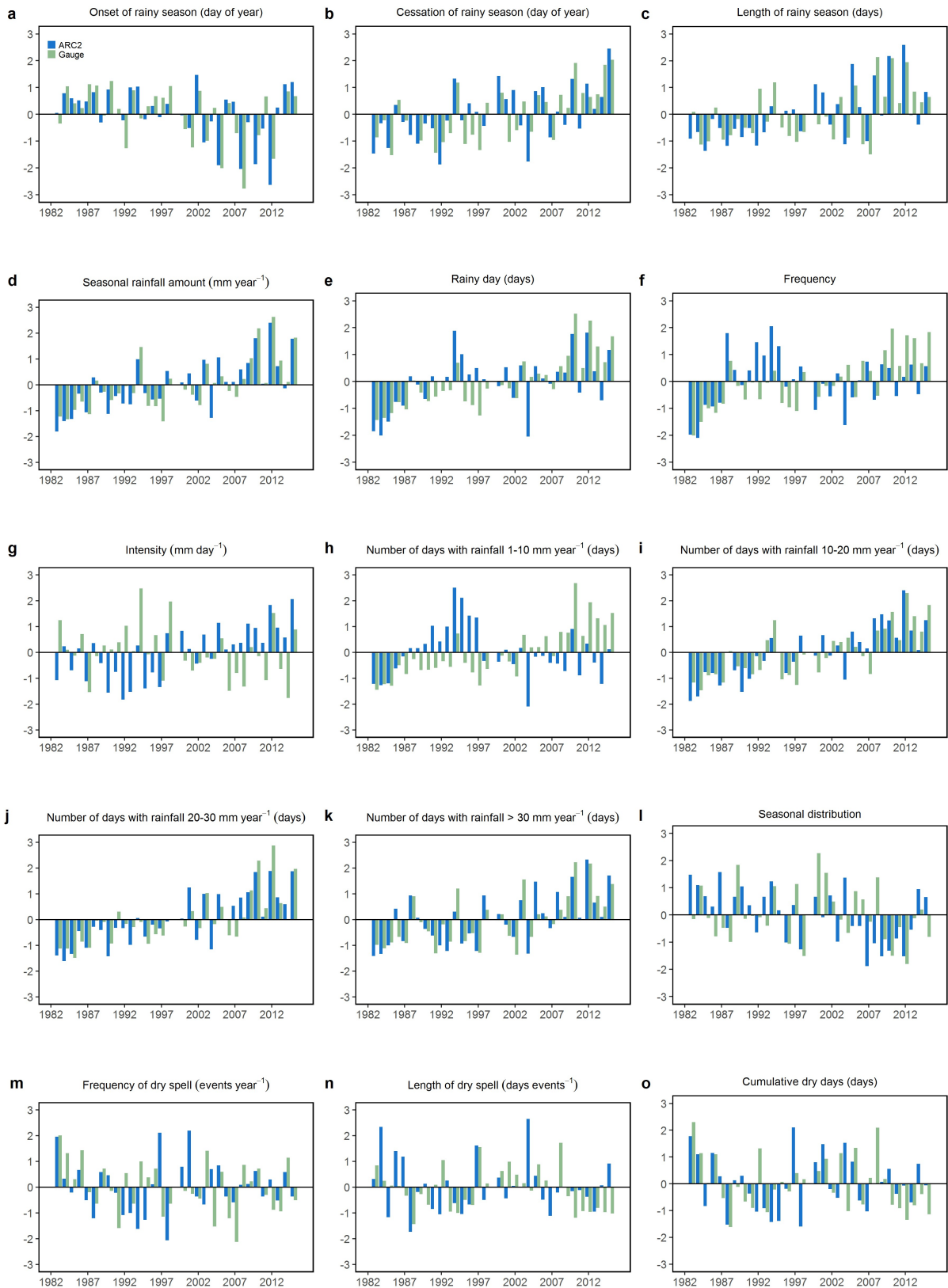
312 and seasonal distribution when end of the time series is around recent years (2007-2015).  
 313 Significantly positive trends are dominating for length of rainy season, seasonal rainfall  
 314 amount, intensity and number of rainy days (10-20, 20-30 and > 30mm day<sup>-1</sup>) for a broad  
 315 array of temporal combinations mirrored by the predominance of negative trends observed  
 316 for the trend in onset of rainy season. Almost no significant trends in dry spells are observed  
 317 regardless of the period of analysis.

318

319 **Table 2** Linear correlation coefficients ( $r$ ) of annual standardized anomalies between ARC2 and rain gauge  
 320 rainfall variables (averages for all gauges and ARC2/MSWEP pixels overlaying rain gauge stations) 1983-2015  
 321 based on Pearson's significance test accounting for temporal autocorrelation. Trends for ARC2, MSWEP and  
 322 gauge variables were estimated using the Sen's slope (*slope*: expressing changes in unit per year). Positive  
 323 (negative) values indicate increasing (decreasing) rainfall variable trends and statistically significant changes  
 324 are denoted by asterisks (\*= $p < 0.1$ ; \*\*= $p < 0.05$ ; \*\*\*= $p < 0.01$ ) with respect to the Mann-Kendall test  
 325 accounting for temporal autocorrelation.

<b>Variables</b>	<b><i>r</i> ARC2- gauge</b>	<b><i>r</i> ARC2- MSWEP</b>	<b><i>trend</i> ARC2</b>	<b><i>trend</i> Gauge</b>	<b><i>trend</i> MSWEP</b>
Onset of rainy season (day of year)	0.67***	0.81***	-0.17*	-0.20**	-0.006
Cessation of rainy season (day of year)	0.49***	0.80***	0.31**	0.33***	0.23**
Length of rainy season (days)	0.57***	0.82***	0.44***	0.51**	0.17**
Seasonal rainfall amount (mm year <sup>-1</sup> )	0.79***	0.90***	5.48***	5.55***	2.41**
Rainy day (days)	0.51**	0.72***	0.21**	0.39***	0.11
Frequency	0.53**	0.68***	0.0005	0.003***	0.0003
Intensity (mm day <sup>-1</sup> )	0.33*	0.36**	0.07***	-0.04	0.03**
Number of days with rainfall 1-10 mm year <sup>-1</sup> (days)	0.23	0.43**	-0.02	0.2***	-0.007
Number of days with rainfall 10-20 mm year <sup>-1</sup> (days)	0.49**	0.79***	0.12***	0.08***	0.09***
Number of days with rainfall 20-30 mm year <sup>-1</sup> (days)	0.69***	0.62***	0.08***	0.05***	0.03*
Number of days with rainfall > 30 mm year <sup>-1</sup> (days)	0.77***	0.78***	0.04***	0.05***	0.008
Seasonal distribution	0.39**	0.49**	-0.01**	-0.004	-0.0002
Frequency of dry spell (events year <sup>-1</sup> )	0.16	0.33*	-0.0001	-0.01	-0.007
Length of dry spell (days events <sup>-1</sup> )	0.06	0.42**	0.001	-0.05	-0.004
Cumulative dry days (days)	0.35*	0.38**	-0.03	-0.18	-0.06

326



327

328

329

330

331

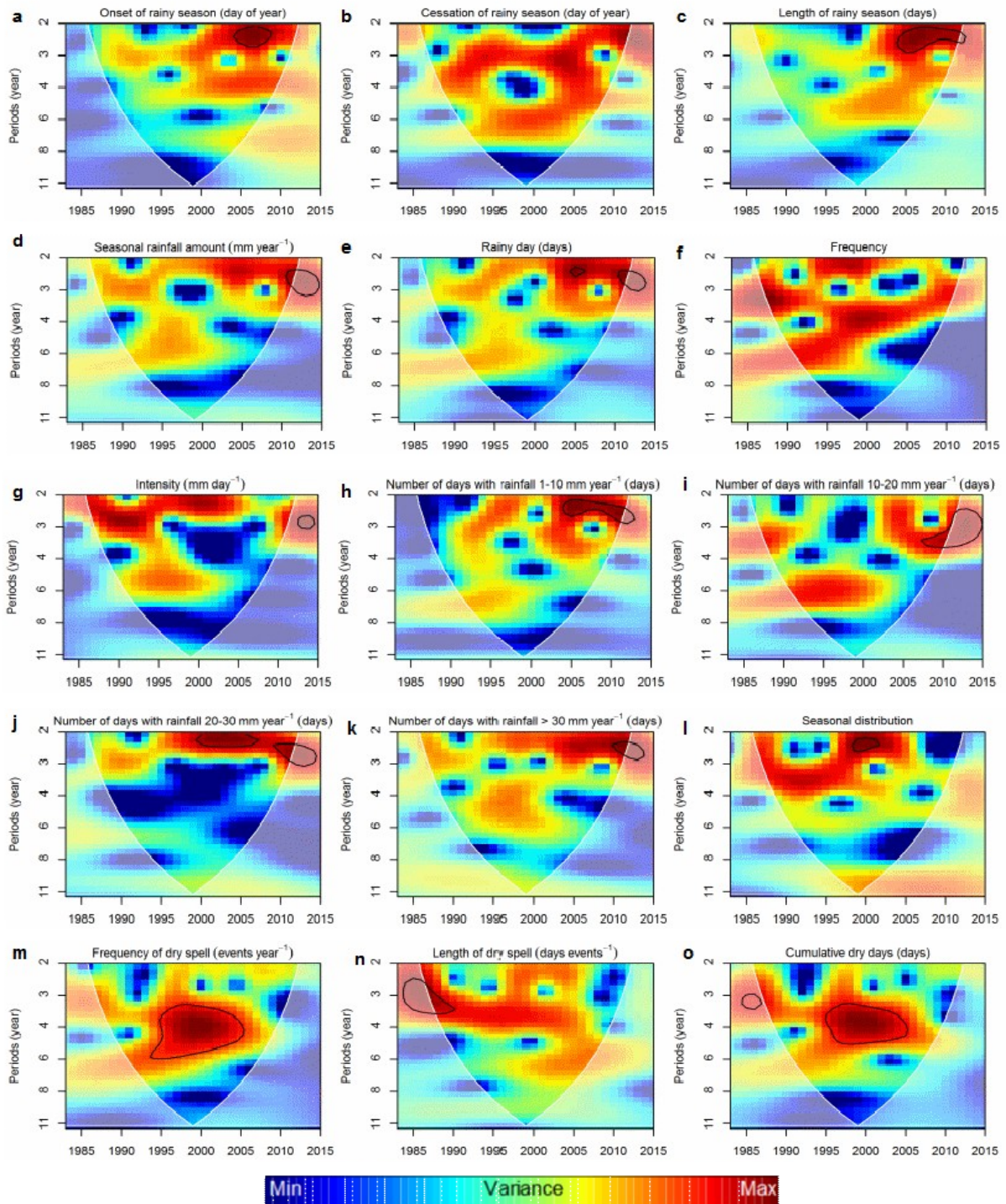
332

333

334

**Fig. 4.** Inter-annual variability in gauge and ARC2 rainfall variables based on annual rainfall anomalies (from the long-term mean 1983-2015). Averages for all gauges and ARC2 pixels overlaying rain gauge stations (Fig. 1). DETAILS: a) onset of rainy season (day of year); b) cessation of rainy season (day of year); c) length of

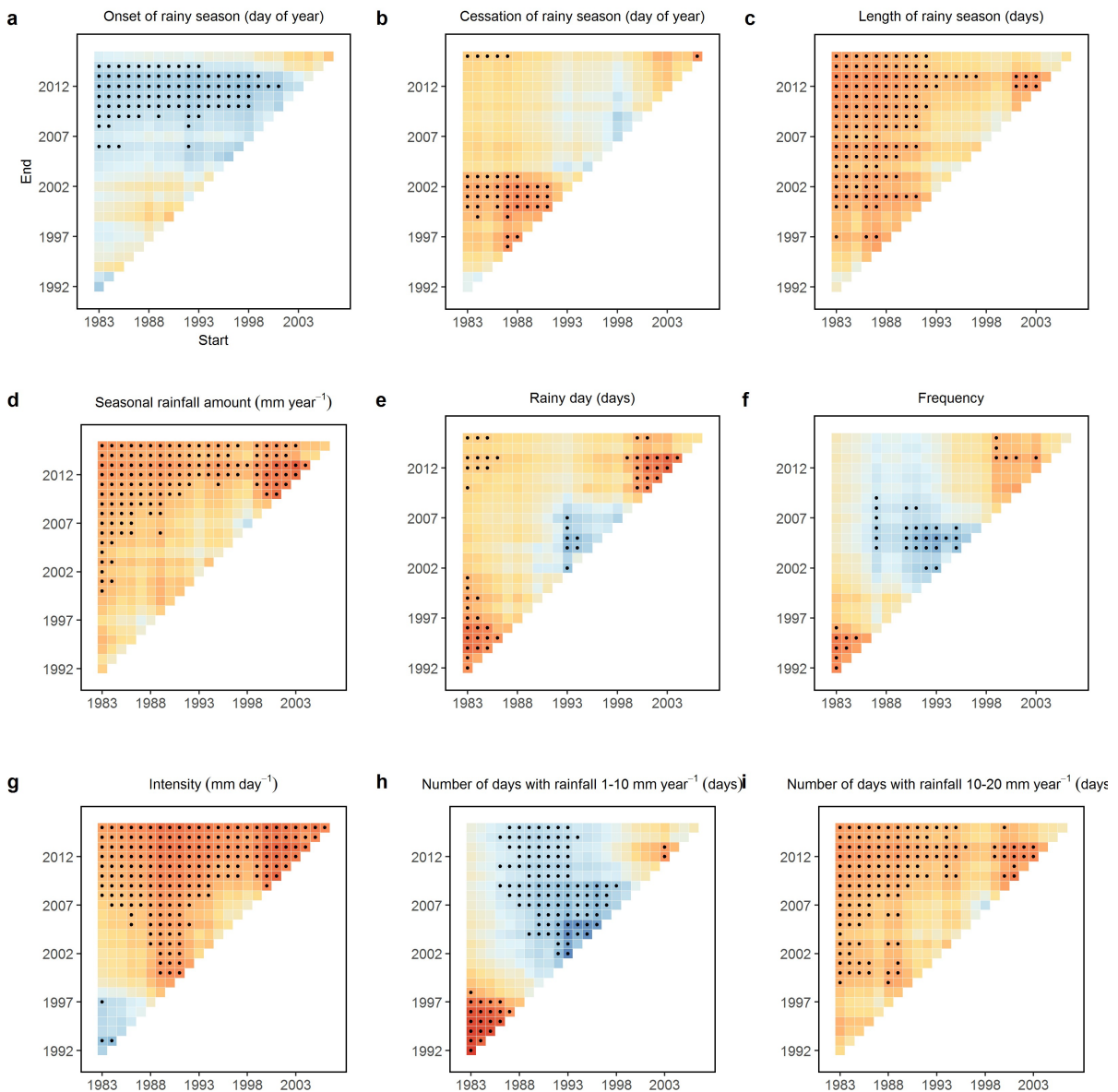
335 rainy season (days); d) seasonal rainfall amount ( $\text{mm year}^{-1}$ ); e) rainy day (days); f) frequency; g) intensity ( $\text{mm}$   
 336  $\text{year}^{-1}$ ); h-k) number of days with rainfall 1-10, 10-20, 20-30,  $>30 \text{ mm day}^{-1}$  (days); l) seasonal distribution; m)  
 337 frequency of dry spell (events  $\text{year}^{-1}$ ); n) length of dry spell (days events $^{-1}$ ); o) cumulative dry days (days).  
 338



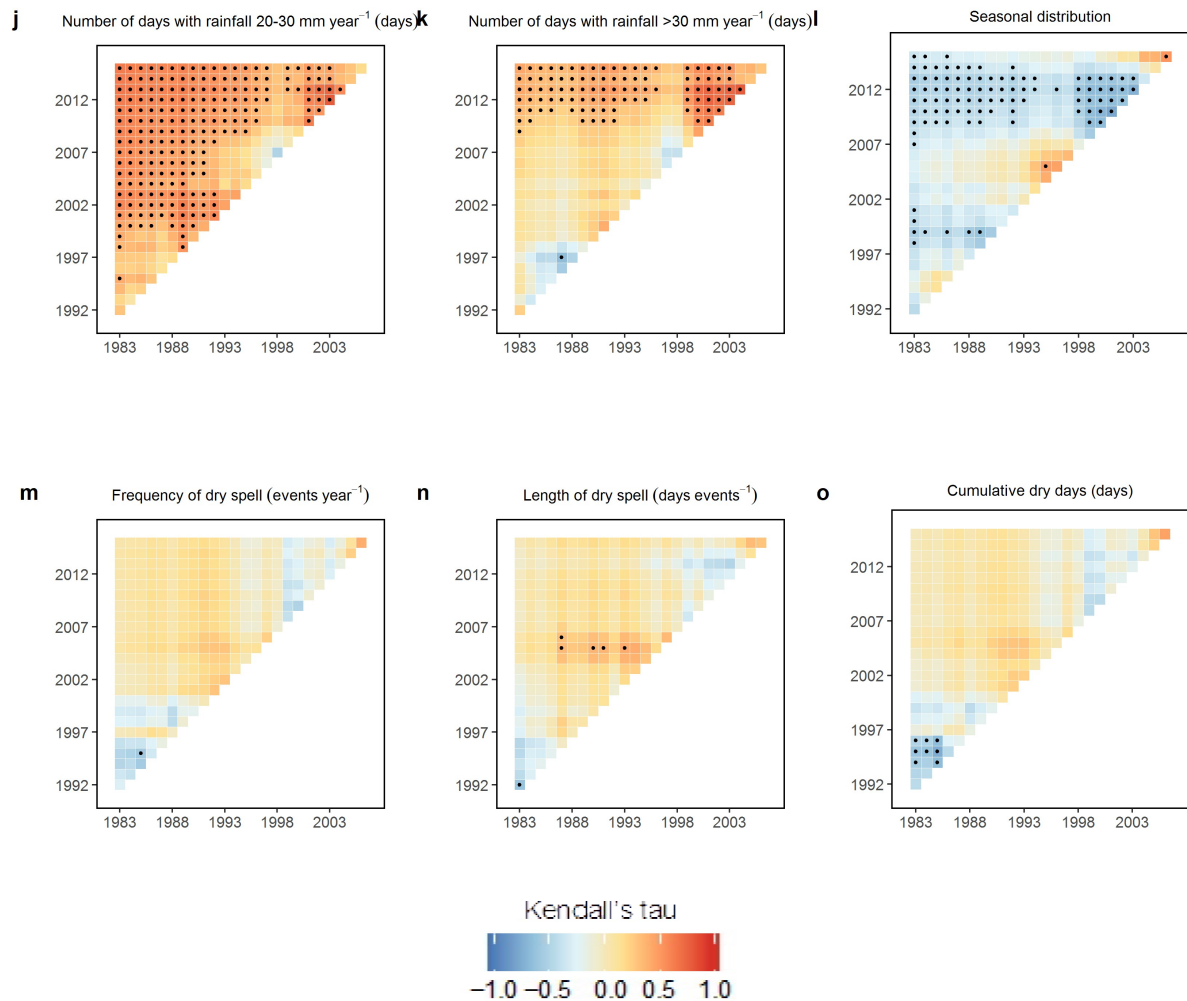
339  
 340 **Fig. 5.** Continuous wavelet power spectrum of annual rainfall variables based on ARC2 rainfall variables  
 341 averaged for 30 pixels overlaying gauges. White lines (the so-called cone of influence) delineate the regions

342 under which power can be underestimated due to edge effects. Black contour lines delimit the regions that are  
 343 statistically significant at the 95% level based on a red noise model [AR(1)] computed for each spectrum as  
 344 described in Torrence and Compo (1998). DETAILS: a) onset of rainy season (day of year); b) cessation of  
 345 rainy season (day of year); c) length of rainy season (days); d) seasonal rainfall amount (mm year<sup>-1</sup>); e) rainy  
 346 day (days); f) frequency; g) intensity (mm year<sup>-1</sup>); h-k) number of days with rainfall 1-10, 10-20, 20-30, >30  
 347 mm day<sup>-1</sup> (days); l) seasonal distribution; m) frequency of dry spell (events year<sup>-1</sup>); n) length of dry spell (days  
 348 events<sup>-1</sup>); o) cumulative dry days (days).

349







353  
354

355

356

357 **Fig. 6.** Trend analysis for ARC2 rainfall variables (average of 30 pixels overlaying gauges) for various periods  
 358 of at least 10 years in length during 1983-2015. The  $x$  and  $y$ -axes indicate the start and ending year,  
 359 respectively. The scale indicates the magnitude of the trend based on Mann–Kendall’s tau coefficient while dots  
 360 mark a significant trend ( $p < 0.05$ ). DETAILS: a) onset of rainy season (day of year); b) cessation of rainy season  
 361 (day of year); c) length of rainy season (days); d) seasonal rainfall amount ( $\text{mm year}^{-1}$ ); e) rainy day (days); f)  
 362 frequency; g) intensity ( $\text{mm year}^{-1}$ ); h-k) number of days with rainfall 1-10, 10-20, 20-30,  $>30 \text{ mm day}^{-1}$  (days);  
 363 l) seasonal distribution; m) frequency of dry spell ( $\text{events year}^{-1}$ ); n) length of dry spell ( $\text{days events}^{-1}$ ); o)  
 364 cumulative dry days (days).

365

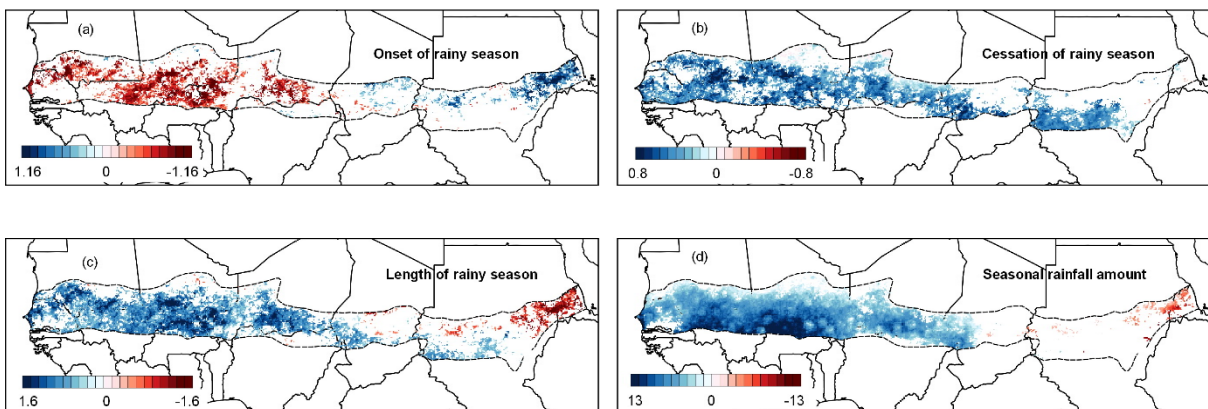
### 366 3.3 Spatio-temporal trends in ARC2 rainfall variables 1983-2015

367 Spatio-temporal trends (linear slope based on Sen’s slope in corresponding unit  $\text{year}^{-1}$ ,  
 368 only significant trends at the 90% confidence level assessed by Mann-Kendall trend test  
 369 accounting for serial correlation are shown) of ARC2 rainfall variables (Table 1) were

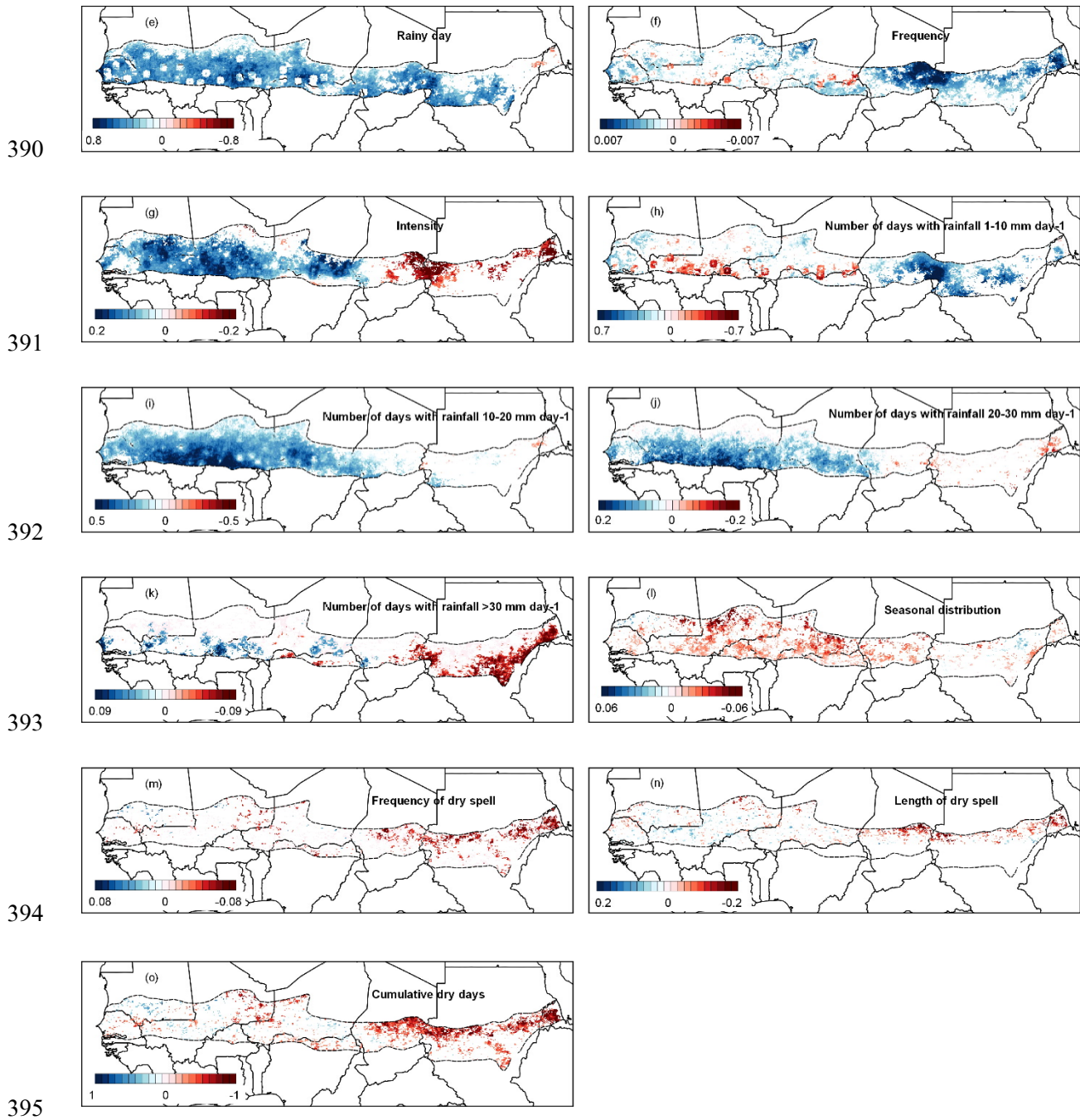
370 calculated for 1983-2015 for the entire Sahel. Rainfall variables of length of the rainy season  
 371 (Fig.7c), the seasonal rainfall amount (Fig.7d), rainy day (Fig.7e), the frequency of rainy  
 372 days (Fig.7f), and the number of days with medium rainfall (10-20 and 20-30 mm day<sup>-1</sup>) and  
 373 to some extent, high rainfall (>30 mm day<sup>-1</sup>) (Fig.7g and i-k) all show positive trends in most  
 374 areas of the western/central Sahel. The longer rainy season in the western/central Sahel seems  
 375 to be associated with an earlier onset date of the rainy season. Much less significant trends  
 376 are seen in the eastern Sahel and some areas even show significantly negative trends;  
 377 especially this is the case for medium and high rainfall events, but also the trends in seasonal  
 378 rainfall and length of the season are negative in some areas of eastern Sahel. The seasonal  
 379 distribution (Fig.7l) generally shows a shift in the ratio between early and late rainfall  
 380 towards later monsoon rainfall from the central part of the Sahel. A scattered pattern of  
 381 negative trends for dry spell characteristics (frequency, length of dry spell, and cumulative  
 382 dry days) are seen primarily in the eastern areas of the Sahel (Fig.7m-o). Trends calculated  
 383 from the number of rainy days, frequency, and the number of days with rainfall 1-10 mm day<sup>-1</sup>  
 384 (Fig.7e, f, and h) include localized spurious circular patterns coinciding with the location of  
 385 rainfall stations. This points towards a data quality issue in the current version of the ARC2  
 386 product related to the use of ground observations for the calibration (see discussion).

387

388



389



396 **Fig. 7.** Trends in ARC2 rainfall variables over Sahel (1983 to 2015) estimated using the Sen's slope (*slope*:  
 397 expressing changes in unit per year). Positive (negative) values indicate increasing (decreasing) rainfall variable  
 398 trends and only statistically significant changes at the 90% confidence level are shown (using Mann-Kendall  
 399 test accounting for temporal autocorrelation). DETAILS: a) onset of rainy season (day of year); b) cessation of  
 400 rainy season (day of year); c) length of rainy season (days); d) seasonal rainfall amount ( $\text{mm year}^{-1}$ ); e) rainy  
 401 day (days); f) frequency; g) intensity ( $\text{mm year}^{-1}$ ); h-k) number of days with rainfall 1-10, 10-20, 20-30, >30  
 402  $\text{mm day}^{-1}$  (days); l) seasonal distribution; m) frequency of dry spell ( $\text{events year}^{-1}$ ); n) length of dry spell (days  
 403  $\text{events}^{-1}$ ); o) cumulative dry days (days).

## 404 **4. Discussion**

### 405 *4.1 Reliability of daily ARC2 rainfall estimates: opportunities and uncertainties*

406 We have shown that a general spatio-temporal consistency exists between rainfall  
407 variables extracted from ARC2, MSWEP and rainfall station data, which can be used to  
408 characterize the rainfall regime in the Sahel. This does not, however, apply to small rainfall  
409 events (especially 1-10 mm day<sup>-1</sup>) (Fig.2h, Fig.S2 and Fig.3h). Estimates in relation to the  
410 number of (small) events are substantially biased between ARC2, MSWEP and gauge  
411 observations with MSWEP showing the highest number of small events and gauge data the  
412 lowest. One plausible explanation could be an inadequacy in the empirically based rainfall  
413 algorithm when correcting for the different scale of measurements. Comparing point based  
414 measurements with satellite estimates representing larger areas (pixels) inevitably leads to a  
415 bias when studying variables with spatial variability (Fensholt et al., 2006). The rainfall of  
416 the Sahel is dominated by localized convective cells, which are likely to cause an  
417 overrepresentation of small rainfall events from satellite (as it is frequently the case that a  
418 small rainfall event will happen somewhere in the  $\approx 121/625$  km<sup>2</sup> (ARC2/MSWEP) pixel, but  
419 not necessarily at the location of the gauge) and vice versa for large events. The difference in  
420 the number of small rainfall events between ARC2/MSWEP and gauge data affects several  
421 variables characterizing the rainfall regime (e.g., intensity, dry spell), where a considerable  
422 bias exists between daily satellite and gauge data. Therefore, a direct comparison between  
423 satellite and gauge rainfall variables influenced by the number of events at the daily time  
424 scale seems less appropriate. This may also be partly responsible for the low correlations  
425 between ARC2 and daily rain gauge rainfall found by Sanogo et al. (2015) and Dembélé and  
426 Zwart (2016). However, even though rainfall variables based on single-day events may be  
427 biased due to the difference in scale of measurements, temporal trends in variables from  
428 satellite and gauge are still expected to be valid for comparison.



429           Several satellite rainfall variables characterizing the sahelian rainfall regime were  
430 found to correlate well with gauge data and therefore do provide important data for areas with  
431 a scarce station network. As very limited rainfall stations provide continuous data in the  
432 Sahel (30 stations were found to match the criteria used in this analysis), the ARC2 data  
433 provide an opportunity for analyzing changes in the rainfall regime. On the other hand,  
434 satellite rainfall estimates are calibrated against gauge data, and the lack of calibration data,  
435 particularly in the eastern Sahel, will inevitably increase the uncertainty of the satellite data,  
436 even though the climatic mechanism causing rainfall is similar between the west and the east  
437 (Sanogo et al., 2015). The consistency between most ARC2 and the global coverage MSWEP  
438 variables (except variables derived directly from single-day events) suggest that rainfall  
439 regime analysis can be conducted for other dryland areas of the world characterized by  
440 convective rainfall systems such as La Plata basin in South America (Nesbitt et al., 2006) or  
441 areas of high spatio-temporal variability like inland Australia and parts of the Middle East  
442 and India (Nicholson, 2011).

443           Artifacts around stations derived from the merging portion of the ARC2 algorithm  
444 typically occur around the dry season, when there are rain signals in the gauge data and zero  
445 rain signals in the satellite information used to define the shape of the rainfall field over space  
446 (personal communication with ARC2 producer Novella, N.). From Fig.7e, f, and h, it is clear  
447 that this issue also extends to the rainy season, which influences rainfall variables being  
448 sensitive to the number of small daily rainfall events (e.g., number of rainy days, number of  
449 rainy days 1-10 mm day<sup>-1</sup>, and frequency). Different trends can be observed around rainfall  
450 gauge sites as compared to the remaining parts of the region, which yields uncertainty for the  
451 reliability of these ARC2 variables. To further investigate the extent of the impact from  
452 artifacts on the consistency between ARC2 and rain gauges (Fig.2 and 4), a comparison was  
453 made for gauge rainfall variables averaged over the rain gauges and all pixels of the

454 western/central Sahel region covering rainfall stations (blue rectangle in Fig.1). Results of  
455 correlations between rain gauges and the ARC2 estimates from pixels covering the entire  
456 region (Fig.S7) are similar to the results of Fig.2 and Fig.S3, confirming that pixels around  
457 rain gauge stations can be used for comparing ARC2 and gauge measurements.

#### 458 *4.2 Implications of rainfall changes 1983-2015*

459         The generally positive trend in ARC2 seasonally summed rainfall for the western and  
460 central Sahel during recent decades (Fig.7d) is well supported by studies based on gauge data  
461 at the monthly or annual scale (Frappart et al., 2009; Lebel and Ali, 2009; Maidment et al.,  
462 2015; Panthou et al., 2014; Sanogo et al., 2015) and other satellite based rainfall products  
463 (Fensholt et al., 2013; Huber et al., 2011; Kaspersen et al., 2011). However, disentangling the  
464 seasonal amount of rainfall into different variables characterizing in more details the rainfall  
465 regime and changes herein, can provide important information for crops and pasture growth.  
466 Our findings show that the increase in annual precipitation is mainly caused by an increase in  
467 rainy days with a longer rainy season (an earlier onset) and especially more days with high  
468 (extreme) rainfall events (Fig.S6), in line with a gauge based study by Panthou et al. (2014),  
469 who also found an increase in inter-annual variability for these variables over the past 15  
470 years. We further observed a shift towards later rainfall at the detriment of early season  
471 rainfall. Changes in the seasonal distribution of rainfall affect the sahelian vegetation as late  
472 rains are of limited use to crops and herbaceous vegetation, and high rain events can have  
473 adverse effects on crop yield and cause increased soil erosion. Moreover, the intra-seasonal  
474 distribution of rainfall impacts the herbaceous mass production and species composition in  
475 any specific year (Diouf et al., 2016). Several studies have shown that the greening of the  
476 Sahel (meaning an increase in net primary productivity monitored by satellites) is strongly  
477 linked to rainfall (Dardel et al., 2014) but cannot be explained by rainfall alone (Fensholt and  
478 Proud, 2012; Herrmann et al., 2005). These studies usually use annual rainfall sums,

479 however, and new insights into changing vegetation patterns and productivity might be  
480 revealed by disentangling seasonal rainfall variables that can be applied at a high spatial  
481 resolution and linked with satellite based vegetation productivity data.

482 At the sub-sahelian scale, we identified areas characterized by an increase in high  
483 rainfall events ( $>30$  mm day<sup>-1</sup>) (e.g. western Senegal, northern Burkina Faso, Southwest  
484 Niger). Also, an earlier start of the rainy season, a longer rainy season, and higher seasonal  
485 amounts were found in the coastal areas of Senegal, in Mali, and in Niger, but not in the  
486 eastern Sahel. Recent studies, based on multi-model analysis, also showed that the summer  
487 precipitation is projected to increase over the central Sahel, but however to decrease over the  
488 western Sahel (2031–2070) as compared to a control period (1960–1999) (Biasutti and Sobel,  
489 2009; James et al., 2015; Monerie et al., 2016). The increase is caused by projected  
490 strengthening of the monsoon circulation leading to a northward shift ultimately producing an  
491 increase of the rainfall amounts in September–October and a delay in the monsoon  
492 withdrawal (Monerie et al., 2016).

493

## 494 **5. Conclusion**

495 Spatio-temporal changes in the sahelian rainfall regime, characterized by the onset,  
496 cessation, and length of the rainy season; seasonal rainfall amount; number of rainy days;  
497 intensity and frequency of rainfall events; and dry spell characteristics, were analyzed from  
498 daily observations using both ARC2 and MSWEP satellite estimates and rain gauge data for  
499 1983-2015. Overall, most rainfall variables estimated from ARC2 were found to be consistent  
500 with station data and the global coverage MSWEP dataset except for the number of daily  
501 observations of small rainfall events ( $< 10$  mm day<sup>-1</sup>). This difference also led to  
502 discrepancies in the estimations of rainfall frequency, intensity, and dry spell characteristics.  
503 Such discrepancies do not, however, impair the results of the ARC2 per-pixel trend analysis

504 of variables based on the number of daily observations per se. Yet, artifacts were found in the  
505 patterns of spatio-temporal trends in ARC2 variables being sensitive to the number of daily  
506 rainfall events, particularly for low rainfall events ( $< 10 \text{ mm day}^{-1}$ ), suggesting that  
507 improvements can be made in the implementation of gauge calibration of the current ARC2  
508 product.

509         Rainfall variables generally showed negative anomalies before the 2000s and positive  
510 anomalies in the later period (except onset, seasonal distribution, and dry spell  
511 characteristics) for both ARC2 and rain gauge data for the western/central Sahel, supporting  
512 the greening of the western/central Sahel over the period 1983-2015. Also, increased inter-  
513 annual variability was observed for most variables since year 2000. Linear trend analysis in  
514 ARC2 rainfall variables characterizing the rainfall regime showed significantly different  
515 patterns between the western/central and eastern Sahel. A strong increase in the seasonal  
516 rainfall, wet season length (caused by both earlier onset and late end), number of rainy days,  
517 and high rainfall events ( $>20 \text{ mm day}^{-1}$ ) was found for the western/central Sahel whereas the  
518 opposite trend characterized the eastern part of the Sahel. Analysis of ARC2 daily rainfall  
519 estimates is concluded to be valuable for improving the understanding of spatio-temporal  
520 trends in the sahelian rainfall regime, albeit with some caution for variables that directly  
521 require calculating the number of daily rainfall events. The consistency between trends in  
522 ARC2 and MSWEP variables suggest that rainfall regime analyses can be conducted for  
523 other dryland areas of the world, where spatio-temporal changes in rainfall are expected to  
524 have profound impacts on livelihoods.

525

## 526 **Acknowledgements**

527         This study is jointly supported by the European Union's Horizon 2020 research and  
528 innovation programme under the Marie Skłodowska-Curie grant agreement (project BICSA

529 number 656564), China Scholarship Council (CSC, 201506190076), and the Danish Council  
530 for Independent Research (DFF) project: Greening of drylands: Towards understanding  
531 ecosystem functioning changes, drivers and impacts on livelihoods. The authors thank  
532 NOAA/NWS/NCEP/ Climate Prediction Center for producing and sharing the Africa Rainfall  
533 Climatology Version 2 (ARC2) datasets and Nicholas Novella for personal communication.  
534 We also thank NOAA National Climatic Data Center for sharing the Global Historical  
535 Climatology Network (GHCN-DAILY) database. Finally, we thank the anonymous  
536 reviewers and editors for their detailed and constructive comments.

537

## 538 **References**

- 539 Adler, R., Huffman, G., Keehn, P., 1994. Global tropical rain estimates from microwave-  
540 adjusted geosynchronous IR data. *Remote Sens. Rev.* 11, 125–152.  
541 doi:10.1080/02757259409532262
- 542 Ali, A., Lebel, T., 2009. The Sahelian standardized rainfall index revisited. *Int. J. Climatol.*  
543 29, 1705–1714. doi:10.1002/joc.1832
- 544 Beck, H.E., van Dijk, A.I.J.M., Levizzani, V., Schellekens, J., Miralles, D.G., Martens, B., de  
545 Roo, A., 2017. MSWEP: 3-hourly 0.25° global gridded precipitation (1979-2015) by  
546 merging gauge, satellite, and reanalysis data. *Hydrol. Earth Syst. Sci. Discuss.* 21, 589–  
547 615. doi:10.5194/hess-21-589-2017
- 548 Berg, A., Quirion, P., Sultan, B., 2009. Weather-index drought insurance in Burkina-Faso:  
549 Assessment of its potential interest to farmers. *Weather. Clim. Soc.* 1, 71–84.  
550 doi:10.1175/2009WCAS1008.1
- 551 Biasutti, M., Sobel, A.H., 2009. Delayed Sahel rainfall and global seasonal cycle in a warmer  
552 climate. *Geophys. Res. Lett.* 36, 1–5. doi:10.1029/2009GL041303
- 553 Breman, H., Kessler, J., 2012. *Woody plants in agro-ecosystems of semi-arid regions: with an*  
554 *emphasis on the Sahelian countries.* Springer Science & Business Media.
- 555 Dardel, C., Kergoat, L., Hiernaux, P., Mougou, E., Grippa, M., Tucker, C.J., 2014. Re-  
556 greening Sahel: 30 years of remote sensing data and field observations (Mali, Niger).  
557 *Remote Sens. Environ.* 140, 350–364. doi:10.1016/j.rse.2013.09.011
- 558 Dembélé, M., Zwart, S.J., 2016. Evaluation and comparison of satellite-based rainfall

559 products in Burkina Faso, West Africa. *Int. J. Remote Sens.* 37, 3995–4014.  
560 doi:10.1080/01431161.2016.1207258

561 Diouf, A.A., Hiernaux, P., Brandt, M., Faye, G., Djaby, B., Diop, M.B., Ndione, J.A.,  
562 Tychon, B., 2016. Do agrometeorological data improve optical satellite-based  
563 estimations of the herbaceous yield in Sahelian semi-arid ecosystems? *Remote Sens.* 8,  
564 668. doi:10.3390/rs8080668

565 Dunning, C.M., Black, E.C.L., Allan, R.P., 2016. The onset and cessation of seasonal rainfall  
566 over Africa. *J. Geophys. Res. Atmos.* 121, 11,405–11,424. doi:10.1002/2016JD025428

567 Durre, I., Menne, M.J., Gleason, B.E., Houston, T.G., Vose, R.S., 2010. Comprehensive  
568 automated quality assurance of daily surface observations. *J. Appl. Meteorol. Climatol.*  
569 49, 1615–1633. doi:10.1175/2010JAMC2375.1

570 Eklund, L., Romankiewicz, C., Brandt, M., Doevenspeck, M., Samimi, C., 2016. Data and  
571 methods in the environment-migration nexus: A scale perspective. *J. Geogr. Soc. Berlin*  
572 147, 139–152. doi:10.12854/erde-147-10

573 Fensholt, R., Proud, S.R., 2012. Evaluation of earth observation based global long term  
574 vegetation trends — Comparing GIMMS and MODIS global NDVI time series. *Remote*  
575 *Sens. Environ.* 119, 131–147. doi:10.1016/j.rse.2011.12.015

576 Fensholt, R., Rasmussen, K., Kaspersen, P., Huber, S., Horion, S., Swinnen, E., 2013.  
577 Assessing land degradation/recovery in the African Sahel from long-term earth  
578 observation based primary productivity and precipitation relationships. *Remote Sens.* 5,  
579 664–686. doi:10.3390/rs5020664

580 Fensholt, R., Sandholt, I., Rasmussen, M.S., Stisen, S., Diouf, A., 2006. Evaluation of  
581 satellite based primary production modelling in the semi-arid Sahel. *Remote Sens.*  
582 *Environ.* 105, 173–188. doi:10.1016/j.rse.2006.06.011

583 Fitzpatrick, R.G.J., Bain, C.L., Knippertz, P., Marsham, J.H., Parker, D.J., 2015. The West  
584 African monsoon onset: A concise comparison of definitions. *J. Clim.* 28, 8673–8694.  
585 doi:10.1175/JCLI-D-15-0265.1

586 Frappart, F., Hiernaux, P., Guichard, F., Mougin, E., Kergoat, L., Arjounin, M., Lavenu, F.,  
587 Koité, M., Paturol, J.-E., Lebel, T., 2009. Rainfall regime across the Sahel band in the  
588 Gourma region, Mali. *J. Hydrol.* 375, 128–142. doi:10.1016/j.jhydrol.2009.03.007

589 Herrmann, S.M., Anyamba, A., Tucker, C.J., 2005. Recent trends in vegetation dynamics in  
590 the African Sahel and their relationship to climate. *Glob. Environ. Chang.* 15, 394–404.  
591 doi:10.1016/j.gloenvcha.2005.08.004

592 Huber, S., Fensholt, R., Rasmussen, K., 2011. Water availability as the driver of vegetation

593 dynamics in the African Sahel from 1982 to 2007. *Glob. Planet. Change* 76, 186–195.  
594 doi:10.1016/j.gloplacha.2011.01.006

595 Hulme, M., 1992. Rainfall changes in Africa: 1931–1960 to 1961–1990. *Int. J. Climatol.* 12,  
596 685–699. doi:10.1002/joc.3370120703

597 Ingram, K.T., Roncoli, M.C., Kirshen, P.H., 2002. Opportunities and constraints for farmers  
598 of west Africa to use seasonal precipitation forecasts with Burkina Faso as a case study.  
599 *Agric. Syst.* 74, 331–349. doi:10.1016/S0308-521X(02)00044-6

600 James, R., Washington, R., Jones, R., 2015. Process-based assessment of an ensemble of  
601 climate projections for West Africa. *J. Geophys. Res.* 120, 1221–1238.  
602 doi:10.1002/2014JD022513.Received

603 Jobard, I., Chopin, F., Bergès, J.C., Roca, R., 2011. An intercomparison of 10-day satellite  
604 precipitation products during West African monsoon. *Int. J. Remote Sens.* 32, 2353–  
605 2376. doi:10.1080/01431161003698286

606 Kaspersen, P.S., Fensholt, R., Huber, S., 2011. A spatiotemporal analysis of climatic drivers  
607 for observed changes in Sahelian vegetation productivity (1982–2007). *Int. J. Geophys.*  
608 2011, 1–14. doi:10.1155/2011/715321

609 Lamb, P.J., 1982. Persistence of Subsaharan drought. *Nat. Clim. Chang.* 299, 46–48.  
610 doi:10.1038/299046a0

611 Laurent, H., D’Amato, N., Lebel, T., 1998. How important is the contribution of the  
612 mesoscale convective complexes to the Sahelian rainfall? *Phys. Chem. Earth* 23, 629–  
613 633. doi:10.1016/S0079-1946(98)00099-8

614 Laurent, H., Jobard, I., Toma, A., 1998. Validation of satellite and ground-based estimates of  
615 precipitation over the Sahel. *Atmos. Res.* 47–48, 651–670.  
616 doi:http://dx.doi.org/10.1016/S0169-8095(98)00051-9

617 Le Barbé, L., Lebel, T., 1997. Rainfall climatology of the HAPEX-Sahel region during the  
618 years 1950–1990. *J. Hydrol.* 188, 43–73. doi:10.1016/S0022-1694(96)03154-X

619 Le Barbé, L., Lebel, T., Tapsoba, D., 2002. Rainfall variability in West Africa during the  
620 years 1950-90. *J. Clim.* 15, 187–202. doi:10.1175/1520-  
621 0442(2002)015<0187:RVIWAD>2.0.CO;2

622 Lebel, T., Ali, A., 2009. Recent trends in the Central and Western Sahel rainfall regime  
623 (1990–2007). *J. Hydrol.* 375, 52–64. doi:10.1016/j.jhydrol.2008.11.030

624 Lebel, T., Cappelaere, B., Galle, S., Hanan, N., Kergoat, L., Levis, S., Vieux, B., Descroix,  
625 L., Gosset, M., Mougin, E., Peugeot, C., Seguis, L., 2009. AMMA-CATCH studies in  
626 the Sahelian region of West-Africa: An overview. *J. Hydrol.* 375, 3–13.

627           doi:10.1016/j.jhydrol.2009.03.020

628   Lebel, T., Diedhiou, A., Laurent, H., 2003. Seasonal cycle and interannual variability of the  
629           Sahelian rainfall at hydrological scales. *J. Geophys. Res. Atmos.* 108, 1401–1411 (and  
630           8389). doi:10.1029/2001JD001580

631   Lebel, T., Taupin, J.D., D’Amato, N., 1997. Rainfall monitoring during HAPEX-Sahel. 1.  
632           General rainfall conditions and climatology. *J. Hydrol.* 188–189, 74–96.  
633           doi:10.1016/S0022-1694(96)03155-1

634   Leisinger, KM, Schmitt, K., 1995. Survival in the Sahel: An ecological and developmental  
635           challenge, International Service for National Agricultural Research.

636   Love, T.B., Kumar, V., Xie, P., Thiaw, W., 2004. A 20-year daily Africa precipitation  
637           climatology using satellite and gauge data, in: *Proceedings of the 84th AMS Annual*  
638           *Meeting, Vol. Conference on Applied Climatology, Seattle, WA–(CD-ROM).*

639   Maidment, R.I., Allan, R.P., Black, E., 2015. Recent observed and simulated changes in  
640           precipitation over Africa. *Geophys. Res. Lett.* 42, 8155–8164.  
641           doi:10.1002/2015GL065765

642   Marteau, R., Moron, V., Philippon, N., 2009. Spatial coherence of monsoon onset over  
643           Western and Central Sahel (1950-2000). *J. Clim.* 22, 1313–1324.  
644           doi:10.1175/2008JCLI2383.1

645   McCollum, J.R., Gruber, A., Ba, M.B., 2000. Discrepancy between gauges and satellite  
646           estimates of rainfall in Equatorial Africa. *J. Appl. Meteorol.* 39, 666–679.  
647           doi:10.1175/1520-0450-39.5.666

648   Menne, M.J., Durre, I., Vose, R.S., Gleason, B.E., Houston, T.G., 2012. An overview of the  
649           global historical climatology network-daily database. *J. Atmos. Ocean. Technol.* 29,  
650           897–910. doi:10.1175/JTECH-D-11-00103.1

651   Monerie, P.A., Biasutti, M., Roucou, P., 2016. On the projected increase of Sahel rainfall  
652           during the late rainy season. *Int. J. Climatol.* 4383, 4373–4383. doi:10.1002/joc.4638

653   Moron, V., 1994. Guinean and Sahelian rainfall anomaly indices at annual and monthly  
654           scales (1933–1990). *Int. J. Climatol.* 14, 325–341. doi:10.1002/joc.3370140306

655   Mortimore, M.J., Adams, W.M., 2001. Farmer adaptation, change and “crisis” in the Sahel.  
656           *Glob. Environ. Chang.* 11, 49–57. doi:10.1016/S0959-3780(00)00044-3

657   Nesbitt, S.W., Cifelli, R., Rutledge, S. a., 2006. Storm morphology and rainfall  
658           characteristics of TRMM precipitation features. *Mon. Weather Rev.* 134, 2702–2721.  
659           doi:10.1175/MWR3200.1

660   Nicholson, S.E., 2011. *Dryland climatology*, Cambridge University Press.



661 doi:10.1029/2012EO390010

662 Nicholson, S.E., 2005. On the question of the “recovery” of the rains in the West African  
663 Sahel. *J. Arid Environ.* 63, 615–641. doi:10.1016/j.jaridenv.2005.03.004

664 Nicholson, S.E., 2000. The nature of rainfall variability over Africa on time scales of decades  
665 to millenia. *Glob. Planet. Change* 26, 137–158. doi:http://dx.doi.org/10.1016/S0921-  
666 8181(00)00040-0

667 Nicholson, S.E., 1993. An overview of African rainfall fluctuations of the last decade. *J.*  
668 *Clim.* 6, 1463–1466. doi:10.1175/1520-0442(1993)006<1463:AOOARF>2.0.CO;2

669 Nicholson, S.E., 1989. Long-term changes in African rainfall. *Weather* 44, 46–56.  
670 doi:10.1002/j.1477-8696.1989.tb06977.x

671 Nicholson, S.E., 1985. Sub-Saharan rainfall 1981-84. *J. Clim. Appl. Meteorol.* 24, 1388–  
672 1391. doi:10.1175/1520-0450(1985)024<1388:SSR>2.0.CO;2

673 Nicholson, S.E., Palao, I.M., 1993. A re-evaluation of rainfall variability in the sahel. Part I.  
674 Characteristics of rainfall fluctuations. *Int. J. Climatol.* 13, 371–389.  
675 doi:10.1002/joc.3370130403

676 Nicholson, S.E., Some, B., McCollum, J., Nelkin, E., Klotter, D., Berte, Y., Diallo, B.M.,  
677 Gaye, I., Kpabeba, G., Ndiaye, O., 2003a. Validation of TRMM and other rainfall  
678 estimates with a high-density gauge dataset for West Africa. Part I: Validation of GPCP  
679 rainfall product and pre-TRMM satellite and blended products. *J. Appl. Meteorol.* 42,  
680 1337–1354. doi:10.1175/1520-0450(2003)042<1355:VOTAOR>2.0.CO;2

681 Nicholson, S.E., Some, B., McCollum, J., Nelkin, E., Klotter, D., Berte, Y., Diallo, B.M.,  
682 Gaye, I., Kpabeba, G., Ndiaye, O., 2003b. Validation of TRMM and other rainfall  
683 estimates with a high-density gauge dataset for West Africa. Part II: Validation of  
684 TRMM rainfall products. *J. Appl. Meteorol.* 42, 1355–1368. doi:10.1175/1520-  
685 0450(2003)042<1355:VOTAOR>2.0.CO;2

686 Novella, N., Thiaw, W., 2012. Africa Rainfall Climatology Version 2. Washingt. Natl.  
687 Ocean. Atmos. Adm.

688 Omotosho, J.B., Balogun, A.A., Ogunjobi, K., 2000. Predicting monthly and seasonal  
689 rainfall, onset and cessation of the rainy season in West Africa using only surface data.  
690 *Int. J. Climatol.* 20, 865–880. doi:10.1002/1097-0088(20000630)20:8<865::AID-  
691 JOC505>3.0.CO;2-R

692 Panthou, G., Vischel, T., Lebel, T., 2014. Recent trends in the regime of extreme rainfall in  
693 the Central Sahel. *Int. J. Climatol.* 34, 3998–4006. doi:10.1002/joc.3984

694 Romankiewicz, C., Doevenspeck, M., Brandt, M., Samimi, C., 2016. Adaptation as by-

695 product: Migration and environmental change in Nguith, Senegal. *J. Geogr. Soc. Berlin*  
696 147, 95–108. doi:10.12854/erde-147-7

697 Sanogo, S., Fink, A.H., Omotosho, J.A., Ba, A., Redl, R., Ermert, V., 2015. Spatio-temporal  
698 characteristics of the recent rainfall recovery in West Africa. *Int. J. Climatol.* 35, 4589–  
699 4605. doi:10.1002/joc.4309

700 Sealy, A., Jenkins, G.S., Walford, S.C., 2003. Seasonal/regional comparisons of rain rates  
701 and rain characteristics in West Africa using TRMM observations. *J. Geophys. Res.*  
702 *Atmos.* 108, 4306. doi:10.1029/2002JD002667

703 Sivakumar, M.V.K., 1989. Agroclimatic aspects of rainfed agriculture in the Sudano-  
704 Sahelian zone. *Soil, Crop. water Manag. Sudano-Sahelian Zo. Proc. an Int. Work.* 17–  
705 38.

706 Sivakumar, M.V.K., 1988. Predicting rainy season potential from the onset of rains in  
707 Southern Sahelian and Sudanian climatic zones of West Africa. *Agric. For. Meteorol.*  
708 42, 295–305. doi:10.1016/0168-1923(88)90039-1

709 Sultan, B., Baron, C., Dingkuhn, M., Sarr, B., 2005. Agricultural impacts of large-scale  
710 variability of the West African monsoon. *Agric. For. Meteorol.* 128, 93–110.  
711 doi:10.1016/j.agrformet.2004.08.005

712 Thorncroft, C.D., Nguyen, H., Zhang, C., Peyrille, P., 2011. Annual cycle of the West  
713 African monsoon: Regional circulations and associated water vapour transport. *Q. J. R.*  
714 *Meteorol. Soc.* 137, 129–147. doi:10.1002/qj.728

715 Torrence, C., Compo, G.P., 1998. A practical guide to wavelet analysis. *Bull. Am. Meteorol.*  
716 *Soc.* 79, 61–78. doi:10.1175/1520-0477(1998)079<0061:APGTWA>2.0.CO;2

717